

The Chemical Evolution of Dwarf Spheroidal Galaxies: Dissecting the Inner Regions and their Stellar Populations

A. Marcolini¹, A. D’Ercole², G. Battaglia^{3,4} and B.K. Gibson^{1,5}

¹ *Centre for Astrophysics, University of Central Lancashire, Preston, Lancashire, PR1 2HE, United Kingdom*

² *Osservatorio Astronomico di Bologna, via Ranzani 1, 40127 Bologna, Italy*

³ *European Organization for Astronomical Research in the Southern Hemisphere, K. Schwarzschild-Str. 2, 85748 Garching, Germany*

⁴ *Kapteyn Institute, University of Groningen, Postbus 800, 9700AV Groningen, the Netherlands*

⁵ *School of Physics, University of Sydney, NSW, 2006, Australia*

Accepted ..., Received ...; in original ...

ABSTRACT

Using 3-dimensional hydrodynamical simulations of isolated dwarf spheroidal galaxies (dSphs), we undertake an analysis of the chemical properties of their inner regions, identifying the respective roles played by Type Ia (SNe Ia) and Type II (SNe II) supernovae. The effect of inhomogeneous pollution from SNe Ia is shown to be prominent within two core radii, with the stars forming therein amounting to $\sim 20\%$ of the total. These stars are relatively iron-rich and α -element-depleted compared to the stars forming in the rest of the galaxy. At odds with the projected stellar velocity dispersion radial profile, the actual 3-dimensional one shows a depression in the central region, where the most metal-rich (ie. $[\text{Fe}/\text{H}]$ -rich) stars are partly segregated. This naturally results in two different stellar populations, with an anti-correlation between $[\text{Fe}/\text{H}]$ and velocity dispersion, in the same sense as that observed in the Sculptor and Fornax dSphs. Because the most iron-rich stars in our model are also the most α -depleted, a natural prediction and test of our model is that the same radial segregation effects should exist between $[\alpha/\text{Fe}]$ and velocity dispersion.

Key words: hydrodynamics - galaxies: dwarf - galaxies: evolution - galaxies: abundances - stars: abundances - Local Group.

1 INTRODUCTION

Hierarchical structure formation models predict that massive galaxies formed through the continuous accretion of numerous satellites, and that such a process, at an admittedly lower rate, should be an ongoing one. Simulations of Milky Way (MW)-like galaxies show stellar halos consisting predominantly of stellar debris from disrupted satellites that is kinematically and spatially distinct from the population of surviving satellites (e.g. Bullock et al. 2001). This is because the survival of a satellite is significantly biased toward outlying lower-mass systems with less eccentric orbits that have fallen into the galaxy at later times (e.g. Moore et al. 2006; Sales et al. 2007). It is not clear if the star formation histories (SFH) and the gas contents of these systems are regulated by internal feedback (e.g. Dekel & Silk 1986) and/or (more likely) by the tidal interaction with the MW and by the ram pressure stripping due to the hot halo of the Galaxy (e.g. Mayer et al. 2006).

If these satellites, or dwarf galaxies, contributed to the build-up of the MW, it becomes fundamentally important to reconstruct how the heavy elements have been produced over

time in *these* systems, in order to understand the evolution of our own Galaxy. With high-resolution spectrographs on 8m-class telescopes, it is now possible to take detailed spectra of individual stars in nearby dwarf galaxies, thereby shedding light on the latter’s chemical enrichment and star formation histories, and consequently, the detailed accounting of the number and type of supernovae that occurred in the past (e.g. Matteucci & Tosi 1985). For this reason, a rich literature exists devoted to studying the chemical evolution of the Galactic satellites. In particular, several authors (e.g. Gilmore & Wyse 1991; Carigi et al. 2002; Ikuta & Arimoto 2002; Lanfranchi & Matteucci 2004, 2007; Robertson et al. 2005; Fenner et al. 2006; Gibson 2007; Carigi & Hernandez 2008) have made chemical models of dwarf spheroidals, employing primarily the assumption of a single-zone framework - i.e., the interstellar medium (ISM) and stellar distributions are assumed to remain homogeneous in space throughout the calculation. As a consequence, spatial inhomogeneities cannot be taken into account by these models, and the values of the inferred chemical and hydrodynamical characteristics can only be interpreted as spatial averages.

Three-dimensional hydrodynamical simulations of the feedback between ISM and SNe within dSph-sized objects have been carried out by Mori et al. (2002) and by Marcolini et al. (2006). Mori et al. (2002) considered pregalactic objects which later merge into galactic halos; in this context, SNe II explode within a few tens of millions of years, their energy efficiently coupled to the ISM in such a manner as to drive an outflow containing a large fraction of the ISM and of the freshly produced metals. Moreover, the rapid timescale over which this outflow is effected ensures a negligible contribution from SNe Ia.¹ On the contrary, the SFHs inferred for surviving dSphs are consistent with being less intense and more prolonged (spanning several Gyrs, in some cases), suggesting that these objects have been able to retain their gas for long periods.

The simulations of Marcolini et al. (2006) accommodated these prolonged SFHs, allowing for the combined effects of both SNe II and SNe Ia. The reason for such an extended SF is due to the effectiveness of radiative losses which contrast the rapid expulsion of gas by SNe II, and leaves it available for SF. As nowadays dSphs have no gas, this scenario requires that the ISM is eventually lost by the interaction with the Galaxy, probably through the combined effects of tidal forces and ram-pressure stripping (e.g. Marcolini et al. 2003; Mayer et al. 2006). Support for this picture is given by the fact that isolated low mass dSphs such as Phoenix (Young et al. 2007) and Leo T (de Jong et al. 2008) were able to form stars up to 100 Myr ago. A further hint in the same direction is given by Haines et al. (2007) who, analysing a sample of $\sim 30,000$ galaxies from the Sloan Digital Sky Survey, found that the SFHs of dwarf galaxies are strongly dependent on their local environment, the fraction of passively evolving galaxies dropping from ~ 70 per cent in dense environments, to zero in the rarefied field.

While the model by Marcolini et al. (2006) represents a noticeable improvement from a hydrodynamical perspective, when compared to traditional one-zone semi-numerical chemical evolution models, it admittedly considered only the elements produced by supernovae. This is not a serious drawback, in the sense that the elements synthesized and distributed by SNe represent a significant fraction of all the elements present today (modulo the contribution from low- and intermediate-mass single stars), and the results of the model can be readily tested against many observational datasets. It has been shown that this model is consistent with many properties of the Draco dwarf (Marcolini et al. 2006) and, with minimal assumptions, the chemical properties of the globular cluster ω -Centauri (Marcolini et al. 2007), which is believed to be the remnant of an ancient dSph.

In the present paper, we analyze the results of the model by Marcolini et al. (2006) focusing on the chemical evolution of the stars located in the central region of dSphs. It has been shown that in several Local Group dSphs, including Sculptor and Fornax, the chemical properties of the stars forming within the galactic core can differ substantially from those situated at larger radii (Tolstoy et al. 2003, 2004; Battaglia et al. 2006). In Section 2, we summarise the char-

acteristics of the Marcolini et al. (2006) simulation. We then discuss our results in Section 3, compare them to observational datasets in Section 4, and draw our conclusions in Section 5.

2 GENERAL PICTURE

Marcolini et al. (2006) carried out three-dimensional hydrodynamical simulations of isolated dSphs, emphasising the different role played by SNe Ia and SNe II in the chemical and dynamical evolution of the system, in the presence of a prolonged intermittent SFH. Although the model has been employed to study the general characteristics of dSphs, it was built initially to explore the origin and evolution of the Draco dSph. In this Section we summarise the main characteristics of the model and its general behaviour. Details of its rationale, as well as the choice of specific parameters, can be found in Marcolini et al. (2006).

2.1 The galaxy model

At first stars are absent, and the galactic potential is given by a static dark halo whose density radial profile (truncated at $r_{h,t}$) is given by:

$$\rho_h(r) = \rho_{h,0} \left[1 + \left(\frac{r}{r_{h,c}} \right)^2 \right]^{-1}. \quad (1)$$

The values of the halo parameters are given in Table 1, and lead to a halo mass $M_h = 6.2 \times 10^7 M_\odot$.

Initially we place the ISM in isothermal equilibrium within the potential well, with a temperature of $T_{\text{ISM}} \sim T_{\text{vir}} = 10^4$ K. The initial gas mass is $M_{\text{ISM}} = 0.18 M_h$, according to the baryonic fraction given by Spergel et al. (2007), which amounts to $1.1 \times 10^7 M_\odot$. The contribution of this baryonic mass to the gravity is neglected.

As the stars form (see next Section), they are randomly distributed in space following a King profile (truncated at $r_{*,t}$):

$$\rho_*(r) = \rho_{*,0} \left[1 + \left(\frac{r}{r_{*,c}} \right)^2 \right]^{-3/2}. \quad (2)$$

After 3 Gyr (the duration of our SFH), a total stellar mass $M_* = 5.6 \times 10^5 M_\odot$ is formed. Assuming a stellar mass to light ratio in the V band $M_*/L_V = 2 M_\odot/L_\odot$, the mass to light ratio inside the stellar tidal radius is $M_\odot/L_{V,\odot} = 80$, in good agreement with observations (e.g. Mateo 1998).

The complete list of parameters concerning the galactic model is given in Table 1. We refer the reader to Marcolini et al. (2006) for a detailed description of the model.

2.2 SFH and SN explosions

The SFH in the model is given by a sequence of 50 instantaneous bursts of identical intensity separated by quiescent periods of 60 Myr. The forming stars are randomly located within the galaxy following the distribution given by Eq. 2.

The SNe II associated to the freshly formed stars explode at a constant rate for a period of 30 Myr (the lifetime

¹ Indeed, SNe Ia are explicitly neglected within the simulations of Mori et al. (2002).

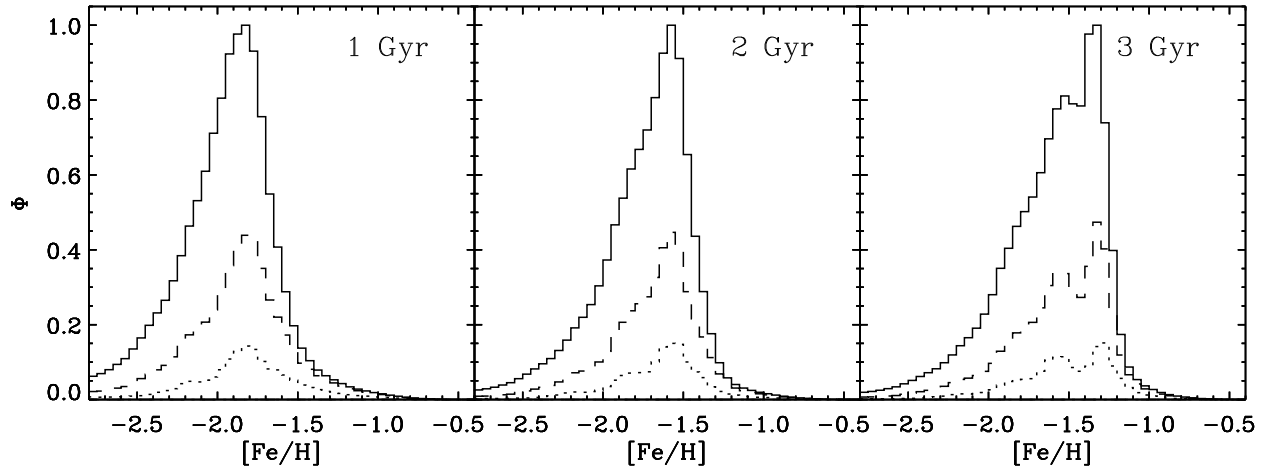


Figure 1. $[\text{Fe}/\text{H}]$ distribution function of the long-lived stars for the “entire dSph volume” (solid line; $r_{*,c} = 130$ and $r_{*,t} = 650$ pc), and within two (dashed line) and one core radii (dotted line), at three different times: 1, 2, and 3 Gyrs, respectively.

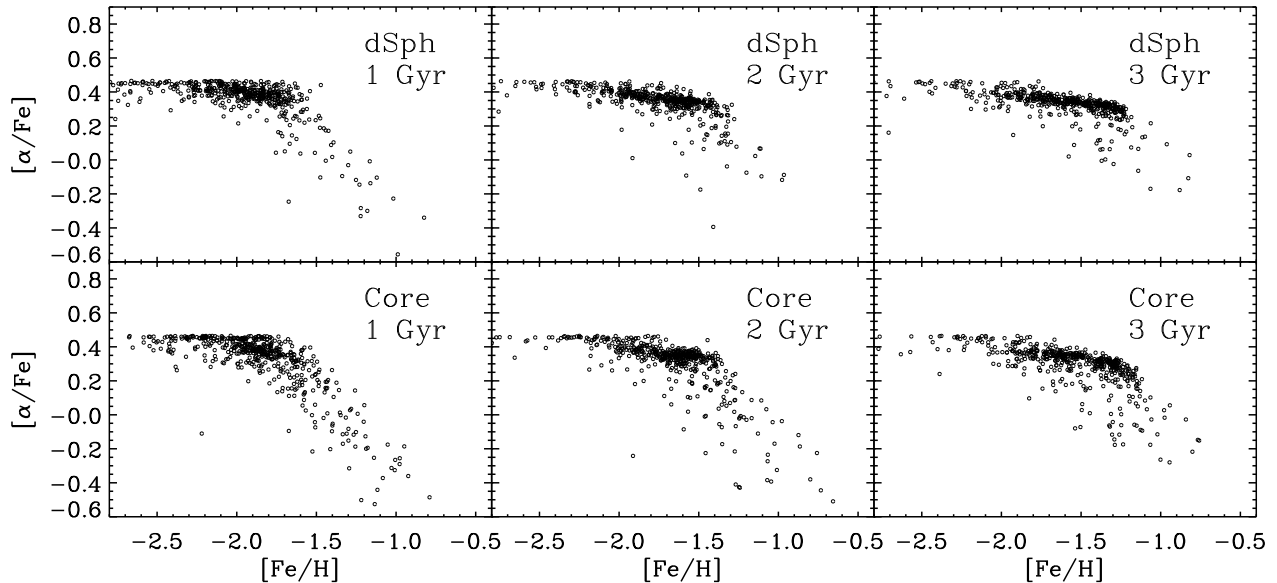


Figure 2. Upper panels: abundance ratio $[\alpha/\text{Fe}]$ versus $[\text{Fe}/\text{H}]$ constructed for a random sample of $N_S = 500$ stars at three different times, for the entire dSph simulated volume. Lower panels: as above, but for stars forming within one core radius. Details on the sampling method are given in footnote 2.

of a $8 M_\odot$ star, the least massive SN II progenitor) after each stellar burst.

The SN Ia rate for a single population decreases in time after an initial rise. We adopted the time-dependent rate given by Matteucci & Recchi (2001), according to the Single-Degenerate scenario.

Each SN explosion is stochastically placed into the galaxy according to its radial probability proportional to the stellar mass within that radius r : $P(r) = M_*(r)/M_*$.

Finally, we assume that each SN II ejects a mean mass $M_{\text{SNII,ej}} = 10 M_\odot$, and each SN Ia ejects $M_{\text{SNIa,ej}} = 1.4 M_\odot$. Every SN II expels $1.0 M_\odot$ of oxygen and $0.07 M_\odot$ of iron while each SN Ia ejects $0.15 M_\odot$ of oxygen and $0.74 M_\odot$

of iron (e.g. Gibson et al. 1997, and reference therein). The explosion energy of each SN of both types is assumed to be $E_{\text{SN}} = 10^{51}$ erg. See Marcolini et al. (2007) for more details of the chemical evolution implementation.

2.3 dSphs evolution

We found that, although the total energy released by the SNe II explosions is larger than the binding energy of the ISM, efficient radiative losses enable the galaxy to retain most of its gas, which thus remains available for the aforementioned prolonged SFH.

Table 1. Galaxy parameters

M_h ($10^6 M_\odot$)	$r_{h,c}$ (pc)	$r_{h,t}$ (pc)	$\rho_{h,0}$ ($10^{-24} \text{ g cm}^{-3}$)	M_\star ($10^5 M_\odot$)	$r_{\star,c}$ (pc)	$r_{\star,t}$ (pc)	$\rho_{\star,0}$ ($10^{-24} \text{ g cm}^{-3}$)	$(M/L_V)_0^a$
62	300	1222	4.3	5.6	130	650	1.0	80

^a Value calculated inside $r_{\star,t}$.

The burst of SNe II associated with each stellar burst pushes the bulk of the ISM to the outskirts of the galaxy. Once the explosions cease (~ 30 Myr after each star burst episode), the ISM flows back towards the centre of the galaxy; when the next burst occurs, the gas is pushed outwards again. This oscillatory behaviour leads to a rather efficient and homogeneous pollution of the ISM by the SNe II ejecta. We note that as the SFH has been fixed *a priori*, it has no direct relation to the gas reservoir within the galaxy. However, stars do form during the quiescent periods between bursts, when the gas has “settled”, and an *a posteriori* consistency for the SFH is recovered. As the galaxy in the present model does not expel the bulk of its ISM, an external cause, such as the interaction with the MW (Mayer et al. 2006), must be invoked at some point during the evolution to deprive the galaxy of its ISM (as the observed Local Group dSphs are essentially devoid of gas).

Given their lower rate, SNe Ia do not significantly affect the general hydrodynamical behaviour of the ISM, but their role is relevant for the chemical evolution of the stars. Because of their longer evolutionary timescales, SNe Ia progenitors created in previous starbursts continue to explode during the subsequent quiescent periods, when the gas is flowing back into the central region. During these periods the higher ambient gas density (together with the lower SNe Ia explosion rate) cause the SNe Ia remnants to be isolated from one another, forming chemically inhomogeneous pockets (hereafter, we refer to these remnants as “SNe Ia pockets”). These pockets are “washed out” by successive phases of expansion and collapse of the ISM, due to the effects of SNe II, but new pockets may form during the quiescent phases between consecutive starbursts. At odd with the ejecta of SNe II, SN Ia debris is rich in iron and deficient in α -elements. Thus, stars forming in the SN Ia pockets possess lower $[\alpha/\text{Fe}]$ ratios and higher $[\text{Fe}/\text{H}]$ ratios than those formed elsewhere. This effect is particularly important for the chemical evolution of the central galactic region, where the SN Ia rate is greater, and higher ambient gas density is achieved.

In the next section we highlight the differences between stars located in the centre and stars located in the outskirts of the galaxy, testing our results against several observational constraints.

3 RESULTS

Although our model was tailored to the Draco dwarf galaxy, it provides a valuable baseline with which to illustrate several generic properties of dSphs.

Figure 1 shows the iron distribution function (IDF) of the long-lived stars (with masses $M < 0.9 M_\odot$) at three different times (1, 2 and 3 Gyrs) for the whole dSph (solid line) and within two (dashed line) and one (dotted line) core

radii. Initially, when the ISM is rather metal-poor, stochastic effects dominate the chemical evolution owing to the still low number of SNs explosions and the inhomogeneous dispersal of their ejecta; as a consequence, the IDF is rather broad and symmetric, as shown in the first panel of the figure. With time, more and more metals pollute the ISM and are homogeneously dispersed by the cyclic behaviour of the gas flow described in the previous section; the newly forming stars are more iron-rich, and the IDF peak moves toward the high-metallicity side of the distribution.

Despite the absence of winds, only $\sim 20\%$ of the SNe ejecta is present within the star forming region. The remainder of the metals, although still gravitationally bound to the galaxy, is driven outwards by the effects of SNe explosions (mimicking, to some degree, an outflow) and does not contaminate the subsequently forming stars.

Even with the homogenising action of SNe II, a degree of inhomogeneous pollution persists due to the newly created SNe Ia pockets; the iron-rich stars forming in such pockets populate the “tail” at high $[\text{Fe}/\text{H}]$ in the IDF. As apparent from Fig. 1, this tail is primarily found within two core radii of the galactic centre, and establishes a chemical difference between the central and outlying stellar populations.

As noted in Section 2, the stars forming in the SNe Ia pockets are characterised, in addition to their higher iron abundance, by their low values of $[\alpha/\text{Fe}]$ (down to ~ -0.5). This is apparent in Fig. 2 which shows the distribution in the $[\alpha/\text{Fe}]-[\text{Fe}/\text{H}]$ plane of a sample of 500 stars representative of the whole stellar population (upper panels) and of the stars within one core radius (lower panels).² As expected, a higher fraction of α -depleted stars is present in the central region, where SNe Ia pockets are preferentially found. Indeed, the fractions of stars with $[\alpha/\text{Fe}] < 0.1$ present after 1 Gyr within one core radius, two core radii, and the entire galaxy are $\sim 20\%$, $\sim 15\%$ and $\sim 10\%$, respectively. These values decrease with time, and at $t = 3$ Gyr they are reduced by a factor $\sim 30\%$. This reduction is due to the decreasing relevance of the contribution of the single pockets, as the mean value of $[\text{Fe}/\text{H}]$ increases with time while the iron content of the pockets is always the same. In fact, from Fig. 2 (as well as from Fig. 1) it is clear that the maximum value of $[\text{Fe}/\text{H}]$ never exceeds ~ -0.7 . Actually, this value is attained by

² One of the outputs of our code at any time is the three-dimensional stellar distribution $\psi(f, o, r)$ (where, for each star, $f \equiv [\text{Fe}/\text{H}]$, $o \equiv [\text{O}/\text{Fe}]$, and r is the position). We can obtain $\Phi(f) = \int dr \int \psi(f, o, r) do$ (shown in Fig. 1) and $\phi(f, o) = \int \psi(f, o, r) dr$. The random sampling shown in Fig. 2 is done as follows: we first extract randomly a value of $[\text{Fe}/\text{H}]$ from the distribution ψ , then a value of $[\alpha/\text{Fe}]$ is randomly extracted from the ϕ distribution calculated for the fixed value of $[\text{Fe}/\text{H}]$. Similar procedures have been followed to obtain the samplings shown in Fig. 3, 4, 6 and 7.

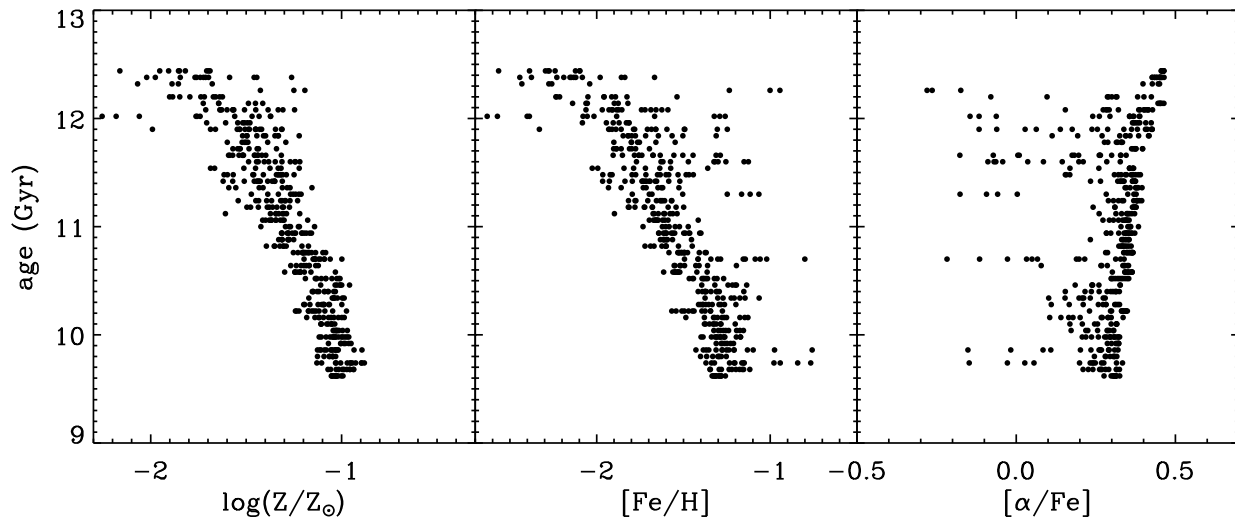


Figure 3. Age- Z , age- $[\text{Fe}/\text{H}]$ and age- $[\alpha/\text{Fe}]$ distributions for 500 sampled stars within one core radius of the simulated volume. Note the metallicity and $[\alpha/\text{Fe}]$ spread amongst coeval stars.

the stars forming within each pocket, where the amount of iron delivered by the SNe Ia is constant ($0.74 M_{\odot}$), and the amount of H does not vary appreciably because the stars form during the quiescent periods, when the ISM settled within the galactic core recovers substantially to the same densities. As a consequence, the maximum obtainable value of $[\text{Fe}/\text{H}]$ is rather insensitive to the ISM mean metallicity, and depends instead on the details of the dSph model. In the particular model we are discussing, the SNe Ia inhomogeneous pollution is expected to become irrelevant at a nearly solar value of $[\text{Fe}/\text{H}]$. The effects of the inhomogeneity are thus expected to be crucial in the metal-poor dwarf galaxies (Marcolini et al. 2007), but not in those more metal-rich.

The stars in Fig. 2 are arranged in two branches, a nearly horizontal plateau and an oblique “ramp” connected to the plateau by a “knee”. The stars located in the upper envelope of the plateau are mostly polluted by the ejecta of SNe II, while the stars below the plateau, as well those on the ramp, are also inhomogeneously (but significantly) polluted in different measure by SNe Ia (see Marcolini et al. 2006, for more details). As the mean iron content of the ISM increases with time, the knee in the $[\alpha/\text{Fe}]-[\text{Fe}/\text{H}]$ diagram moves rightward (toward larger values of $[\text{Fe}/\text{H}]$) and, to a lesser extent, downward (to lower $[\alpha/\text{Fe}]$).

A further evidence of the inhomogeneous pollution is given in Fig. 3, where we plot the age- $\log(Z/Z_{\odot})$, age- $[\text{Fe}/\text{H}]$ and age- $[\alpha/\text{Fe}]$ relations for a randomly-drawn sample of 500 stars formed within one core radius. In the first two panels a striking spread in the metallicity Z and in the iron content of the star is apparent, which tends to reduce with time, as expected. The $[\text{Fe}/\text{H}]$ spread is more accentuated because stars formed inside SNe Ia pockets have a much higher iron content, but essentially the same Z , than the stars formed elsewhere, since SNe Ia deliver a significant amount of iron but a negligible fraction of metals in comparison to SNe II (for example, after 3 Gyr the SNe Ia ejecta accounts for 30% of the iron produced by all stars, but only for 2% of the metals).

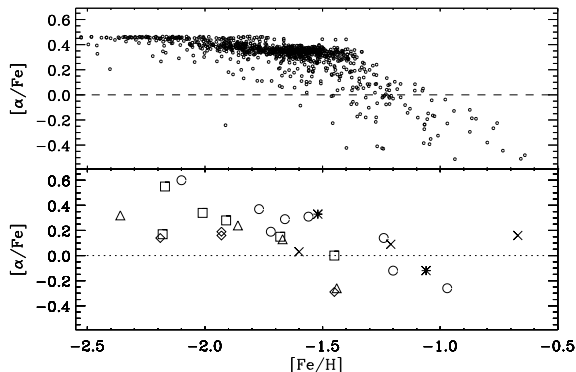


Figure 4. Abundance ratio $[\alpha/\text{Fe}]$ versus $[\text{Fe}/\text{H}]$ for 500 sampled stars of the reference model at $t = 2$ Gyr, compared to a dataset of 28 dSph stars (Draco: triangles ; Fornax: crosses; Leo I: asterisks; Sextans: diamonds; Sculptor: circles; Ursa Minor: squares) collected from the literature (see text for details). The stars are sampled as in Fig. 2.

It is commonplace to assume that stars have chemical elements in solar proportion, thus leading to an implicit equivalence between the IDF and the metal distribution function (MDF). That said, a comparison between the first two panels of Fig. 3 indicates that the two distributions are different (see Marcolini et al. 2007, for more details about this point and how it influences the color-magnitude diagrams).

Finally, the third panel of Fig. 3 illustrates the evolution of $[\alpha/\text{Fe}]$ and shows that the SNe Ia pockets start to form quite early in the evolution (~ 300 Myr after the first star formation episode, as the SNe Ia rate starts to become appreciable) and the tendency of its spread to decrease with time (see also the lower panels of Fig. 2).

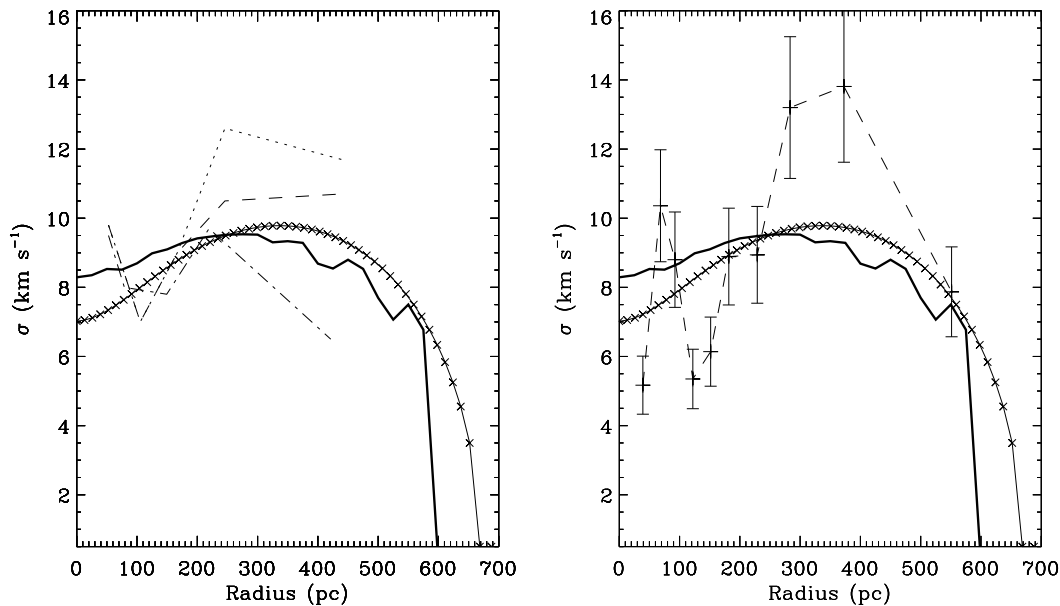


Figure 5. The radial profile of the 3D velocity dispersion (solid line with crosses) and projected velocity dispersion using 1000 sampled stars of our model (thick solid line) obtained solving the Jeans-equation compared to the velocity dispersion of Draco dSph obtained by Lokas et al. (2005, left panel) for three samples of 207 (dotted), 203 (dashed) and 189 (dash-dotted) stars, and compared to the velocity dispersion obtained by Muñoz et al. (2005, right panel).

4 COMPARISON WITH DATA

In Fig. 4, we compare the chemical characteristics of the stars of the model (at 2 Gyr) with data published by several authors (Shetrone et al. 2001, 2003; Tolstoy et al. 2003; Geisler et al. 2005) for different dSphs (Draco, Fornax, Leo I, Sextans, Sculptor and Ursa Minor) observed using VLT/UVES.

Although the dataset is a collection of values of different dSphs, the general pattern of the observed $[\alpha/\text{Fe}]$ - $[\text{Fe}/\text{H}]$ diagram is reproduced quite well by our single model. Due to the small number statistics in published results it is difficult to draw definitive conclusions. Tolstoy et al. (2003) suggested that the similar abundance patterns across several dSph galaxies was evidence for very similar chemical evolution histories, similar initial conditions and similar initial mass functions, despite their different SFHs, although there is also evidence for differences (Venn et al. 2004; Tolstoy et al. 2006; Letarte et al. 2007). Larger samples coming from FLAMES high resolution data sets should make this issue clearer (Hill et al. in prep; Venn et al. in prep), greatly increasing the statistics inside each single galaxy, including the Sculptor and Fornax dSphs. Indeed, one should compare the model with a dataset for *each* dwarf galaxy as the corresponding “knee” can start at different $[\text{Fe}/\text{H}]$ values depending upon the chemical enrichment history of the dSph citeptolstoy2006,latarte2007. However, for the aim of this paper, the literature data are sufficient to highlight the main characteristics (note that the future larger samples will overlay the present UVES sample). Here, we simply wish to highlight the point that α -depleted stars are observed in several dSphs, just as predicted by the model.

Actually, α -depleted stars can also be explained within the framework of the chemical model of Lanfranchi & Matteucci (2004, 2007), in which the $[\alpha/\text{Fe}]$ decrease at larger values of $[\text{Fe}/\text{H}]$ is the consequence of a galactic wind which reduces the amount of available gas; the formation of new stars is thus tempered, along with the α -elements delivered by SNe II. SNe Ia, instead, having progenitors with longer evolutionary timescales (Matteucci & Greggio 1986), continue to inject iron into the ISM, lowering the $[\alpha/\text{Fe}]$ ratio of the gas. In this case the α -depleted stars should be the youngest ones, with the largest values of $[\text{Fe}/\text{H}]$, and exhibiting a small spread in age. Preliminary results of $[\alpha/\text{Fe}]$ measurements of ~ 90 stars in Sculptor and ~ 55 stars in Fornax recently published by Tolstoy et al. (2006) seem to indicate that α -depleted stars are found at any $[\text{Fe}/\text{H}] > -1.8$ down to $[\text{Fe}/\text{H}] \sim -0.6$ inside each galaxy, in good agreement with our model.

In Fig. 5 the projected radial velocity dispersion profiles of the model are plotted and tested against data inferred for Draco by Muñoz et al. (2005) and Lokas et al. (2005). The velocity dispersion profile is calculated solving the Jeans equation and assuming velocity isotropy ($\beta = 0$). Different choices of the β parameter can change the results dramatically, even if there is no valid motivation, *a priori*, for choosing highly tangential or radial orbits; as such, $\beta = 0$ appears a fair conservative value. For example Mateo et al. (2007) found that for Leo I stars, those situated more towards the centre appear to have isotropic kinematics, while only those located outside a “break radius” of about 500 pc exhibit significant velocity anisotropy. These authors also suggest that the break radius represents the location of the tidal radius of Leo I.

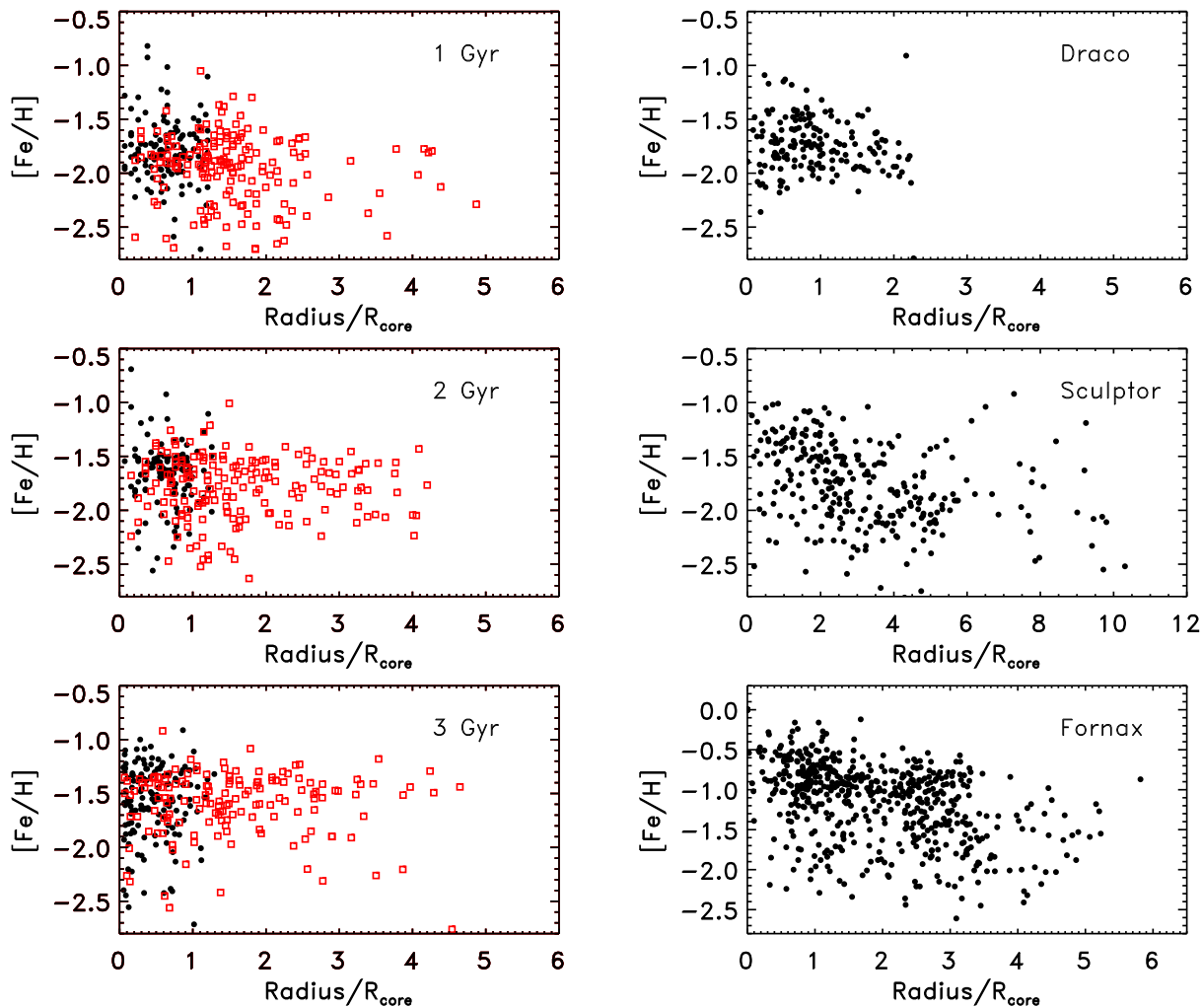


Figure 6. Left panels: $[\text{Fe}/\text{H}]$ projected radial distributions of 300 sampled stars at three different times (1, 2 and 3 Gyr). Right panels: observed $[\text{Fe}/\text{H}]$ radial distributions for 87 stars in Draco (Faria et al. 2007), 308 stars in Sculptor (Tolstoy et al. 2004) and 562 stars in Fornax (Battaglia et al. 2006). The empty squares represent stars with $\sigma > 8.5 \text{ km s}^{-1}$ while black dots are stars with $\sigma < 8.5 \text{ km s}^{-1}$.

In the same figure, we also plot the actual 3D velocity dispersion profile within the galaxy (solid line with crosses). While the projected profile is essentially flat (within 1 km s^{-1}) up to 500 pc, the actual profile shows a central minimum, $\sim 3 \text{ km s}^{-1}$ below the maximum value attained in the outer regions. The tendency of the central stars of the model to have somewhat lower values of the velocity dispersion is emphasised in the left panels of Fig. 6, where we show the projected radial positions and the ratios $[\text{Fe}/\text{H}]$ of a sample of 300 stars: here the empty squares represent stars with $\sigma > 8.5 \text{ km s}^{-1}$ while black dots are stars with $\sigma < 8.5 \text{ km s}^{-1}$. These diagrams also show that $[\text{Fe}/\text{H}]$ rich stars are found preferentially in the central region of the system (and only with lower velocity dispersion), while the main Fe-poor population is more smoothly distributed. This result can be easily understood: while the iron-rich stars form preferentially in the SNe Ia pockets which are more concentrated toward the center, the stars with lower values of $[\text{Fe}/\text{H}]$ form throughout the galaxy from an ISM whose pollution does not depend strongly on the radius because of the dynamically-driven homogenisation (cf. Section 2). As

a consequence, two different stellar populations are found in our model, with iron-poor stars showing higher velocity dispersion and iron-rich (centrally concentrated) stars showing lower velocity dispersion. A similar anti-correlation between the iron content and the velocity dispersion has been actually observed in Sculptor (Tolstoy et al. 2004) and Fornax (Battaglia et al. 2006) dSphs (and found in preliminary models that we adapted to these galaxies).

From the left panels in Fig. 6 it is apparent that the metallicity gradients occurring in our model are rather small, at variance with monolithic dissipative models of elliptical galaxy formation. In these models strong gradients form as a consequence of existing radial flows carrying inward the heavy elements produced in the outer regions (Larson 1974). In our model, instead, because of the small size of dSphs, the gas flows powered by the SNe II tend to homogenize the ISM, thus inhibiting the formation of chemical gradients (cf. section 2); the present mild $[\text{Fe}/\text{H}]$ gradient is mainly due to SNe Ia, as discussed in 3. Indeed, being that the oxygen (and α -elements in general) is produced for the most part

by SNe II, the $[\text{O}/\text{H}]$ gradient is even shallower than that of $[\text{Fe}/\text{H}]$ (Marcolini et al. 2006).

From the left panels in Fig. 6 it is also apparent that the small metallicity gradient (0.2-0.4 dex; see Marcolini et al. 2006) tends to decrease with time as the amount of iron in the ISM increases and the stars forming at larger radii acquire increasing values of $[\text{Fe}/\text{H}]$. This tendency seems to be confirmed by the stellar radial distributions of Draco (Faria et al. 2007), Sculptor (Tolstoy et al. 2004) and Fornax (Battaglia et al. 2006) (right panels in Fig. 6): these dSphs seem to possess shallower gradients, as their SFH (e.g. Buonanno et al. 1999; Dolphin 2002; Tolstoy et al. 2003, and reference therein) is more prolonged. While this behaviour can be described only qualitatively by the reference model of Marcolini et al. (2006), further models tailored to Sculptor and Fornax are planned, in order provide a more appropriate and direct comparison to the data. Nevertheless, our model seems to be in good agreement with the “central concentration” of the “small $[\text{Fe}/\text{H}]$ tail” found by Faria et al. (2007) for Draco.

We stress that the presence in the galactic center of an iron-rich stellar population could be explained in principle also by other models. In the framework depicted by Mori et al. (2002) the SNe feedback following the initial star formation blows out the gas and stops star formation temporarily. After SNe feedback becomes weaker, more metal-rich gas can return and form a new generation of stars distributed closer to the center. As pointed out in Section 1, however, the model of Mori et al. (2002) is not suitable in the case of the prolonged SFHs often encountered in dSphs. A more metal rich central population of stars is also obtained in the model of Kawata et al. (2006) as the result of a steep metallicity gradient within a single population, induced by dissipative collapse of the gas component. This is the same mechanism that is suggested to explain the metallicity gradient for larger spheroidals, i.e. normal elliptical galaxies. It is interesting to note that in these galaxies the observed gradient of $[\alpha/\text{Fe}]$ has a mean value close to zero, and that it does not correlate with galactic properties (e.g. Sánchez-Blázquez et al. 2007; Pipino et al. 2007). Thus, within the scheme proposed by Kawata et al. (2006), dSphs are not expected to present a well defined $[\alpha/\text{Fe}]$ gradient. On the contrary, in the model of Marcolini et al. (2006) α -depleted stars are centrally segregated (see Fig. 7) as they are correlated with the Fe-rich stars which are preferentially found in the central region. Thus the observations of the $[\alpha/\text{Fe}]$ radial profile in dSphs can potentially select between the model of Marcolini et al. (2006) and the scheme proposed by Kawata et al. (2006). As an aside, the model of Marcolini et al. (2006) also predicts that the most α -depleted stars have lower velocity dispersions, as illustrated in Fig. 7.

We point out that, although the proximity of the MW may change the stellar orbits (especially in the outskirts) of a local dSph, a segregation of the α -depleted stars should still be present because such stars are located within two core radii, a region only slightly affected by the tidal interaction (e.g. Gao et al. 2004; Peñarrubia et al. 2008).

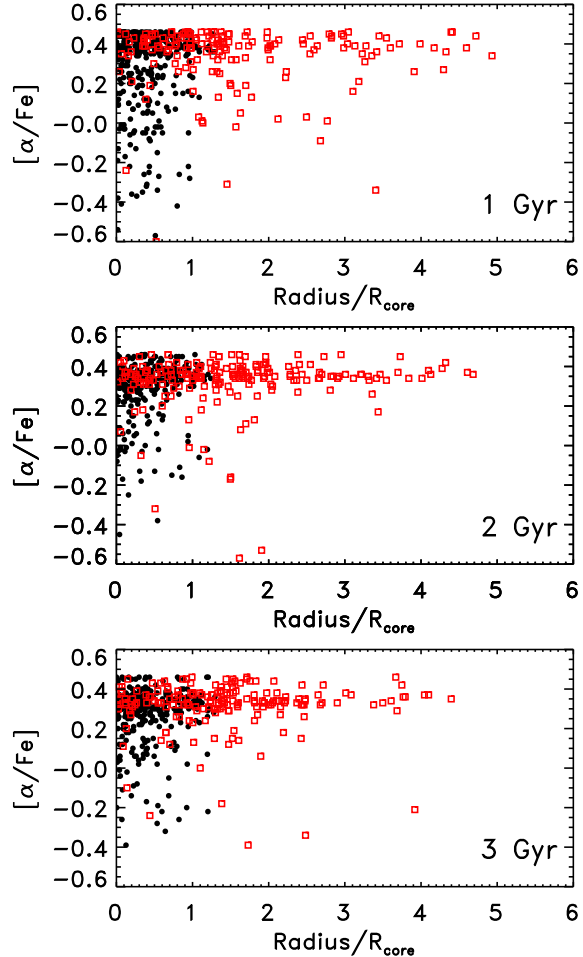


Figure 7. $[\alpha/\text{Fe}]$ projected radial distributions of 500 sampled stars at three different times (1, 2 and 3 Gyr). The empty squares represent stars with $\sigma > 8.5 \text{ km s}^{-1}$ while black dots are stars with $\sigma < 8.5 \text{ km s}^{-1}$.

5 CONCLUSIONS

We analysed the outcome of the 3D hydrodynamical model of the Draco dSph of Marcolini et al. (2006), and found that the results can provide a useful, if qualitative, description of the larger population of generic Local Group dSphs. We can summarise our major findings as follows:

i) Evidence is mounting about the effects of inhomogeneous pollution on the chemical history of the stars in dSphs (Koch et al. 2008). The effect of the inhomogeneous pollution of SNe Ia found in Marcolini et al. (2006) is more important in the central region (within two core radii) of dSphs. Here the stars forming in the SNe Ia pockets can amount to $\sim 20\%$ of the total.

ii) The chemical homogenisation of the ISM by SNe II, together with the combined inhomogeneous pollution by SNe Ia, naturally accounts for a radial segregation of Fe-rich stars (with depleted $[\alpha/\text{Fe}]$ ratios) in the central regions of dSphs. Stars with this abundance pattern have been observed in the center of several dSphs (Shetrone et al. 2001, 2003; Bonifacio et al. 2004; Monaco et al. 2005; Tolstoy et al. 2006; Koch et al. 2008). As discussed, the most Fe-rich stars in our model are also

α -depleted, and thus the same radial segregation should be observed to test and prove our model.

iii) At odd with the projected stellar velocity dispersion radial profile, the actual one shows a depression in the central region, where the iron-rich stars are partly segregated. This naturally entails two different stellar populations with an anti-correlation between [Fe/H] and velocity dispersion, which has been observed in the case of the Sculptor dSph (Tolstoy et al. 2004) and the Fornax dSph (Battaglia et al. 2006).

In a forthcoming paper we will compare new simulations tailored to specific dSphs (e.g. Fornax and Sculptor) with the properties of hundreds of stars observed with VLT-FLAMES that will be available soon (Venn & Hill 2005; Tolstoy et al. 2006, and references therein). The new models will take into account the yields from low- and intermediate-mass asymptotic giant branch stars, as well as the interaction with our Galaxy, in order to describe how the dSphs lose their gas. For example, an interaction with the MW seems to be particularly important in the evolution of the Sagittarius dwarf. Preliminary results show that the iron-rich, α -depleted stars in this galaxy are consistent with a SF strongly affected by this interaction, as well as with the formation *in situ* of M54 as the core of this galaxy.

ACKNOWLEDGMENTS

We thank the anonymous referee for his/her useful comments that improved the presentation of the paper. We also kindly thank Eline Tolstoy for reading the manuscript and for useful discussion, we are also in debt with Ricardo Muñoz for giving us the data to make Fig. 5. This research was undertaken as part of the Commonwealth Cosmology Initiative (CCI:www.thecci.org). AD acknowledges financial support from National Institute for Astrophysics (INAF). The simulations were run at the CINECA Supercomputing Centre, and supported through the award of grant from INAF-CINECA. Analysis has been undertaken at the UCLan HPC Facility.

REFERENCES

- Battaglia G., Tolstoy E., Helmi A., Irwin M. J., Letarte B., Jablonka P., Hill V., Venn K. A., Shetrone M. D., Arimoto N., Primas F., Kaufer A., Francois P., Szeifert T., Abel T., Sadakane K., 2006, *A&A*, 459, 423
- Bonifacio P., Sbordone L., Marconi G., Pasquini L., Hill V., 2004, *A&A*, 414, 503
- Bullock J. S., Kravtsov A. V., Weinberg D. H., 2001, *ApJ*, 548, 33
- Buonanno R., Corsi C. E., Castellani M., Marconi G., Fusi Pecci F., Zinn R., 1999, *AJ*, 118, 1671
- Carigi L., Hernandez X., 2008, *astro-ph/08021203*, 802
- Carigi L., Hernandez X., Gilmore G., 2002, *MNRAS*, 334, 117
- de Jong J. T. A., Harris J., Coleman M. G., Martin N. F., Bell E. F., Rix H., Hill J. M., Skillman E. D., Sand D. J., Olszewski E. W., Zaritsky D., Thompson D., Giallongo E., Ragazzoni R., DiPaola A., Farinato J., Testa V., Bechtold J., 2008, *astro-ph/08014027*, 801
- Dekel A., Silk J., 1986, *ApJ*, 303, 39
- Dolphin A. E., 2002, *MNRAS*, 332, 91
- Faria D., Feltzing S., Lundström I., Gilmore G., Wahlgren G. M., Ardeberg A., Linde P., 2007, *A&A*, 465, 357
- Fenner Y., Gibson B. K., Gallino R., Lugaro M., 2006, *ApJ*, 646, 184
- Gao L., De Lucia G., White S. D. M., Jenkins A., 2004, *MNRAS*, 352, L1
- Geisler D., Smith V. V., Wallerstein G., Gonzalez G., Charbonnel C., 2005, *AJ*, 129, 1428
- Gibson B. K., 2007, in *IAU Symposium Vol. 241 of IAU Symposium, The Chemistry of the Local Group*. pp 161–164
- Gibson B. K., Loewenstein M., Mushotzky R. F., 1997, *MNRAS*, 290, 623
- Gilmore G., Wyse R. F. G., 1991, *ApJ*, 367, L55
- Haines C. P., Gargiulo A., La Barbera F., Mercurio A., Merluzzi P., Busarello G., 2007, *MNRAS*, 381, 7
- Ikuta C., Arimoto N., 2002, *A&A*, 391, 55, (IA)
- Kawata D., Arimoto N., Cen R., Gibson B. K., 2006, *ApJ*, 641, 785
- Koch A., Grebel E. K., Gilmore G. F., Wyse R. F. G., Kleya J. T., Harbeck D. R., Wilkinson M. I., Evans N. W., 2008, *astro-ph/08022104*
- Lanfranchi G. A., Matteucci F., 2004, *MNRAS*, 351, 1338
- Lanfranchi G. A., Matteucci F., 2007, *A&A*, 468, 927
- Larson R. B., 1974, *MNRAS*, 166, 585
- Letarte B., Hill V., Tolstoy E., 2007, in *EAS Publications Series Vol. 24 of EAS Publications Series, Chemical Analysis of Fornax dwarf spheroidal with VLT/FLAMES*. pp 33–38
- Lokas E. L., Mamon G. A., Prada F., 2005, *MNRAS*, 363, 918
- Marcolini A., Brighenti F., D’Ercole A., 2003, *MNRAS*, 345, 1329
- Marcolini A., D’Ercole A., Brighenti F., Recchi S., 2006, *MNRAS*, 371, 643
- Marcolini A., Sollima A., D’Ercole A., Gibson B. K., Ferraro F. R., 2007, *MNRAS*, 382, 443
- Mateo M., Olszewski E. W., Walker M. G., 2007, *astro-ph/07081327*
- Mateo M. L., 1998, *ARA&A*, 36, 435
- Matteucci F., Greggio L., 1986, *A&A*, 154, 279
- Matteucci F., Recchi S., 2001, *ApJ*, 558, 351
- Matteucci F., Tosi M., 1985, *MNRAS*, 217, 391
- Mayer L., Mastropietro C., Wadsley J., Stadel J., Moore B., 2006, *MNRAS*, 369, 1021
- Monaco L., Bellazzini M., Bonifacio P., Ferraro F. R., Marconi G., Pancino E., Sbordone L., Zaggia S., 2005, *A&A*, 441, 141
- Moore B., Diemand J., Madau P., Zemp M., Stadel J., 2006, *MNRAS*, 368, 563
- Mori M., Ferrara A., Madau P., 2002, *ApJ*, 571, 40
- Muñoz R. R., Frinchaboy P. M., Majewski S. R., Kuhn J. R., Chou M.-Y., Palma C., Sohn S. T., Patterson R. J., Siegel M. H., 2005, *ApJ*, 631, L137
- Peñarrubia J., Navarro J. F., McConnachie A. W., 2008, *ApJ*, 673, 226
- Pipino A., Matteucci F., D’Ercole A., 2007, *astro-ph/07090658*
- Robertson B., Bullock J. S., Font A. S., Johnston K. V., Hernquist L., 2005, *ApJ*, 632, 872

- Sales L. V., Navarro J. F., Abadi M. G., Steinmetz M., 2007, MNRAS, 379, 1464
- Sánchez-Blázquez P., Forbes D. A., Strader J., Brodie J., Proctor R., 2007, MNRAS, 377, 759
- Shetrone M., Venn K. A., Tolstoy E., Primas F., Hill V., Kaufer A., 2003, AJ, 125, 684
- Shetrone M. D., Côté P., Sargent W. L. W., 2001, ApJ, 548, 592
- Spergel D. N., Bean R., Doré O., Nolta M. R., Bennett C. L., Dunkley J., Hinshaw G., Jarosik N., Komatsu E., Page L., Peiris H. V., Verde L., Halpern M., Hill R. S., Kogut A., Limon M., Meyer S. S., Odegard N., Tucker G. S., 2007, ApJS, 170, 377
- Tolstoy E., Hill V., Irwin M., Helmi A., Battaglia G., Letarte B., Venn K., Jablonka P., Shetrone M., Arimoto N., Abel T., Primas F., Kaufer A., Szeifert T., Francois P., Sadakane K., 2006, The Messenger, 123, 33
- Tolstoy E., Irwin M. J., Helmi A., Battaglia G., Jablonka P., Hill V., Venn K. A., Shetrone M. D., Letarte B., Cole A. A., Primas F., Francois P., Arimoto N., Sadakane K., Kaufer A., Szeifert T., Abel T., 2004, ApJ, 617, L119
- Tolstoy E., Venn K. A., Shetrone M., Primas F., Hill V., Kaufer A., Szeifert T., 2003, AJ, 125, 707
- Venn K. A., Hill V., 2005, in Hill V., François P., Primas F., eds, From Lithium to Uranium: Elemental Tracers of Early Cosmic Evolution Vol. 228 of IAU Symposium, Chemistry of Stars in the Sculptor Dwarf Galaxy from VLT-FLAMES. pp 513–518
- Venn K. A., Irwin M., Shetrone M. D., Tout C. A., Hill V., Tolstoy E., 2004, AJ, 128, 1177
- Young L. M., Skillman E. D., Weisz D. R., Dolphin A. E., 2007, ApJ, 659, 331